






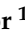





Article

Assessing Economic Complementarity in Wind–Solar Hybrid Power Plants Connected to the Brazilian Grid

Rafael B. S. Veras ^{1,*} , Clóvis B. M. Oliveira ¹ , Shigeaki L. de Lima ¹ , Osvaldo R. Saavedra ¹ ,
Denisson Q. Oliveira ¹ , Felipe M. Pimenta ² , Denivaldo C. P. Lopes ¹ , Audálio R. Torres Junior ^{1,3} ,
Francisco L. A. Neto ⁴ , Ramon M. de Freitas ⁵  and Arcilan T. Assireu ⁶ 

¹ Institute of Electrical Energy, Federal University of Maranhão, Av. dos Portugueses s/n, São Luís 65080-040, MA, Brazil

² Center for Physical and Mathematical Sciences, Postgraduate Program in Oceanography, Trindade Campus, Federal University of Santa Catarina, Florianópolis 88040-900, SC, Brazil

³ Postgraduate Program in Oceanography, Federal University of Maranhão, Av. dos Portugueses s/n, São Luís 65080-040, MA, Brazil

⁴ Laboratory of Applied Meteorology, Federal University of Rio de Janeiro, Rio de Janeiro 21941-916, RJ, Brazil

⁵ Camargo Schubert Wind Engineering, Rua Juvenal Galeno-55, Curitiba 82520-030, PR, Brazil

⁶ Institute of Natural Resources, Federal University of Itajubá, Av. BPS 1303, Pinheirinho, Itajubá 37500-903, MG, Brazil

* Correspondence: rafael.brito@discente.ufma.br

Abstract: The share of electricity generation from Variable Renewable Energy Sources (VRES) has increased over the last 20 years. Despite promoting the decarbonization of the energy mix, these sources bring negative characteristics to the energy mix, such as power ramps, load mismatch, unpredictability, and fluctuation. One of the ways to mitigate these characteristics is the hybridization of power plants. This paper evaluates the benefits of hybridizing a plant using an AI-based methodology for optimizing the wind–solar ratio based on the Brazilian regulatory system. For this study, the hybrid plant was modeled using data collected over a period of 10 months. The measurements were obtained using two wind profilers (LIDAR and SODAR) and a sun tracker (Solys 2) as part of the EOSOLAR R&D project conducted in the state of Maranhão, Brazil. After the power plant modeling, a Genetic Algorithm (GA) was used to determine the optimal wind–solar ratio, considering costs with transmission systems. The algorithm achieved a monthly profit increase of more than 39% with an energy curtailment inferior to 1%, which indicates economic complementarity. Later, the same methodology was also applied to verify the wind–solar ratio’s sensitivity to solar energy pricing. The results show that a price increase of 15% would change the power plant’s optimal configuration.

Keywords: wind power; solar power; hybrid power plants; optimization; economic complementarity; Maranhão state; Brazil Interconnected System



Citation: Veras, R.B.S.; Oliveira, C.B.M.; de Lima, S.L.; Saavedra, O.R.; Oliveira, D.Q.; Pimenta, F.M.; Lopes, D.C.P.; Torres Junior, A.R.; Neto, F.L.A.; de Freitas, R.M.; et al. Assessing Economic Complementarity in Wind–Solar Hybrid Power Plants Connected to the Brazilian Grid. *Sustainability* **2023**, *15*, 8862. <https://doi.org/10.3390/su15118862>

Academic Editors: Doug Arent, Adam Warren and Xiaolei Yang

Received: 25 March 2023

Revised: 17 May 2023

Accepted: 24 May 2023

Published: 31 May 2023



Copyright: © 2023 by the authors. Licensee MDPI, Basel, Switzerland. This article is an open access article distributed under the terms and conditions of the Creative Commons Attribution (CC BY) license (<https://creativecommons.org/licenses/by/4.0/>).

1. Introduction

Over the past two decades, the global installed capacity of wind and solar power has grown from 18 GW to over 1.4 TW. The installed power of these technologies added together today is 77 times greater than 25 years ago [1].

Despite promoting the decarbonization of the energy mix, due to their intermittent, variable, stochastic, and unpredictable behavior, these sources bring negative characteristics to the electricity system. The higher the rate of Variable Renewable Energy Sources (VRES) in a system, the higher the complexity of its operation.

Several ways to mitigate these negative characteristics are addressed in the literature. The most common one is the use of storage systems. Works [2–5] applied strategies that use energy storage to approach this problem. They obtained results that point to a dramatic reduction in the variability, fluctuation, and ramp rate of grid-connected VRES power plants when coupled with Battery Energy Storage Systems (BESS).

Besides energy storage, other strategies are addressed by researchers. In work [6], the authors carried out a comprehensive review of methods and techniques to mitigate the mismatch between demand and renewable energy generation. This paper explores the positive effects that the aggregation of multiple VRES, from the same or different sources, brings to the system in reducing variability.

The aggregation of renewable energy generation plants stands out because it requires fewer resources besides the conversion devices from the sources and the transmission lines. This strategy is widely studied in power systems and is called energy complementarity. It consists of the use of one or more sources with intermittent behavior that are different from each other and that complement each other in time or space. The first studies exploring the positive effects of combining one or more energy sources with complementary characteristics date back to 1978 [7]. However, the topic has been gaining more importance since 2016, proving real benefits to the system [8].

As VRES have variable behavior, the generation curve will hardly satisfy the load curve. The solution to this problem, especially in isolated systems, is usually the use of storage systems. Due to the high cost of BESS, this aspect can often make it financially unfeasible to implement the project. Works [9–11] propose a strategy of diversifying VRES in a system to increase load follow-up. The results achieved imply a drastic reduction in the need and expense for storage systems when source diversification is employed, and this strategy also presents the potential for greater integration of VRES into large-scale systems without imposing excessive strain on the power system's flexibility to manage the variability of these sources [12].

Another negative aspect of VRES discussed in the studies is the intermittency of the sources. This characteristic leads to an imprecise predictability of generation due to a significant number of ramps, which can occur due to cloud coverage passing over solar panels or even sudden turbulent wind variations at a microscale in a wind farm. Some of the studies analyzed address complementarity as a means to smooth the power output curve of generation projects and mitigate this aspect. In [13–15], three VRES with different variability characteristics are utilized. These studies demonstrate that diversifying energy resources results in smoother, more uniform and predictable power generation curves. Additionally, ref. [16] emphasizes the advantage of tidal energy as a complementary source, as it exhibits better intermittent characteristics than solar energy. Tidal energy, particularly in locations with semi-diurnal tides, displays four daily peaks, offering reduced intermittency, improved predictability, and consistently available energy in a more uniform manner.

An additional important topic addressed in the literature is the optimal share of sources in the composition of a hybrid system. Some papers have applied AI techniques to determine this optimal combination of wind and solar power in hybrid plants, but with different objectives. For instance, ref. [17] worked on the minimization of power ramps and fluctuations, while [18] focused on evaluating the economic feasibility of repowering old wind parks with solar energy. The results of both works suggest that the optimal proportion between the sources varies depending on the power and load conditions, the climatic conditions, and most importantly, the final objective of the mix (e.g., reducing costs or increasing energy production).

One notable finding in the studies on this topic is the variation in correlation between energy sources depending on the location. In the study conducted by [15], which evaluated the complementarity between wind, solar, and hydroelectric sources in Rio de Janeiro, it was found that the correlation coefficient indicates low complementarity between wind and solar sources in this specific location. Conversely, in the study by [19], which explored complementarity between these same two sources across the entire European continent, coefficients close to -1 were discovered, indicating high complementarity between the sources. Therefore, it is evident that local studies are necessary to determine the extent of complementarity among available energy sources in a specific location.

This type of complementarity explored within the same location is known in the literature as temporal complementarity, while when hybridization is evaluated across different

locations, it is referred to as spatial complementarity [20]. In fact, studies such as [21–24] highlight that, as the distance between energy sources increases, their complementarity improves. This characteristic can be leveraged to mitigate the variability of VRES in large interconnected systems.

Considering these benefits for the system, hybrid power plants are becoming more popular in global electricity markets. In the United States alone, in 2019, the installed capacity of hybrid plants totaled 13.4 GW, divided into 125 enterprises with various configurations among wind, solar, hydroelectric, biomass, geothermal, coal, and batteries [25]. Meanwhile, on the Asian continent, China holds the record for the largest hybrid enterprise in the world: namely, the Longyangxia hydro-solar power plant, with a power capacity of 2.13 GW, 1.28 GW hydroelectric, and 0.85 GW solar.

The authors of [26] considered the transmission system in their assessment of complementarity. This article not only demonstrates the correlation between energy sources but also explores the technical feasibility of a potential generation project by analyzing the distance between the energy sources comprising the hybrid plant and the transmission system for power evacuation. A problem that is not well addressed in the literature is the connection to the transmission system. This is because these sources have variable behavior, and they can generate power equal to their maximum capacity in one specific hour, and fall off to zero in the next one. This aspect causes great inefficiency in the use and contracting of transmission systems.

Therefore, this study aims to propose a method for evaluating the complementarity of wind–solar grid-connected hybrid systems. Because the area of interest is situated in a coastal equatorial region, wind and solar energy sources are likely to have a positive correlation coefficient. This is typically unfavorable for energy complementarity. In this region, the temperature difference between the surfaces of the sea and the continent increases near noon. This high temperature gradient establishes atmospheric pressure gradients responsible for the onset of the sea breeze, which coincides with a high rate of solar radiance. As the wind speed accelerates at the same time that the solar radiation peaks, positive correlation coefficients between these two sources are expected for this region.

Due to the expected presence of positive correlation coefficients, this study aims to investigate what is referred to here as economic complementarity; i.e., when, taking into consideration local regulations, one or more sources complement each other, bringing economic benefits or advantages to the power generation system entrepreneur, even for energy resources with a positive or near-zero correlation coefficient. An optimization method will be used in accordance with local regulations for the use of the transmission system. The goal is to minimize transmission costs while maximizing profits from energy sales. The generation of both primary energy sources used in this study was calculated using data from a 12-month measurement campaign. Wind and solar data were collected in Maranhão, Brazil, through the EOSOLAR R&D project using LIDAR and SODAR wind profilers and the Solys 2 sun tracker. Finally, it will be verified whether the regulatory conditions in the country are capable of stimulating the VRES hybrid power plant market in the equatorial region through economic complementarity.

2. Access to the Transmission System

Transmission system charging practices differ widely across the world [27]. In Brazil, the Contracts of Use of the Transmission System (CUST) are mainly regulated by the Brazilian National Electric Energy Agency (ANEEL) through normative resolution REN 666/2015. This specifies that the Transmission System Amount of Use (TSAU), in MW, contracted by the plant for a period of 4 years, is the value of the maximum injectable power in the transmission system, which must be at least equal to the installed power subtracted from the minimum own load. The Transmission System Use Charge (TSUC) will then be the value of the TSAU multiplied by the Transmission System Use Fee (TSUF), in BRL/MW, as described in Equation (1). Because this regulation is applied in the Brazilian electricity

sector, the TUSF unit is BRL/MW, but it can be transformed to any currency by applying the exchange rate.

$$\text{TSUC} [\$] = \text{TSUF} \left[\frac{\$}{\text{MW}} \right] \cdot \text{TSAU} [\text{MW}] \quad (1)$$

The requirement of a TSAU equal to the installed power discourages the establishment of VRES power plants, because the intermittent characteristic of these sources causes TSUCs to be inefficient and the grid to have many idle periods, which is negative for the environment and for the generation and transmission system investors. One solution to mitigate the inefficiency of CUSTs would be to hybridize the plant by means of complementary sources.

Aiming to promote the establishment of hybrid projects in Brazil and thus take advantage of the positive characteristics that they bring to the system, ANEEL homologated the normative resolution REN 954/2021 in November 2021. The three topics relevant to this work that this regulation addresses are:

- The concept of a Hybrid Power Plant (HPP) as an installation for electric power production from the combination of different generation technologies, with distinct measurements per technology or not and licensed in a single process;
- The concept of power band, corresponding to the interval between the nominal power of the predominant energy source and the total sum of all sources included in the generation plant. In an HPP, the TSAU is equal to the power band, which is defined by the user.
- The possibility of an annual reduction in value of 5% of the TSAU to compensate for climate seasonality.

3. Materials and Methods

The case study in this paper is performed using data measured on-site. The wind and solar data come from field measurements performed by the EOSOLAR project through November 2021 and November 2022 in a region called Pequenos Lençóis, near the city of Paulino Neves, in the state of Maranhão, Brazil. EOSOLAR is an R&D project led by the Federal University of Maranhão and fully funded by private initiatives. The main objectives of this project were the development of the wind and solar atlas of the state of Maranhão, and other research in the field of wind energy and turbulence [28,29]. The measurement station was installed about 2.5 km from the Delta III wind farm complex. This is a joint complex of 15 wind farms totaling a capacity of 426 MW. Figure 1 highlights, with a red circle, the site where the measurements took place, and each turbine that composes the Delta III complex is marked by a blue point. This location was chosen due to its suitability for an examination of the wind and solar potential, because its landscape is predominantly marked by gentle slopes, and also because it contains the wind characteristics of the wind farm without, however, being affected by the wakes generated by the wind turbines.

3.1. Wind Data

The wind dataset for the EOSOLAR project was acquired by remote sensing, using a LIDAR (Light Detection and Ranging) model Windcube V2, manufactured by Vaisala in Vantaa, Finland, a SODAR model MFAS manufactured by Scintec in Rottenburg am Neckar, Germany, and also two 10 m micro meteorological towers, each containing three 2D sonic anemometers (5 m, 7.5 m and 10 m), and one 3D anemometer (3.5 m). Both LIDAR and SODAR (seen in Figure 2A,B) were set up to take samples every 10 m in height from 40 to 200 m for the LIDAR, and every 10m in height from 30 to 280 m for the SODAR.



Figure 1. Measurement site, with the station highlighted in red and the wind generators of the Delta III wind farm illustrated by blue dots.

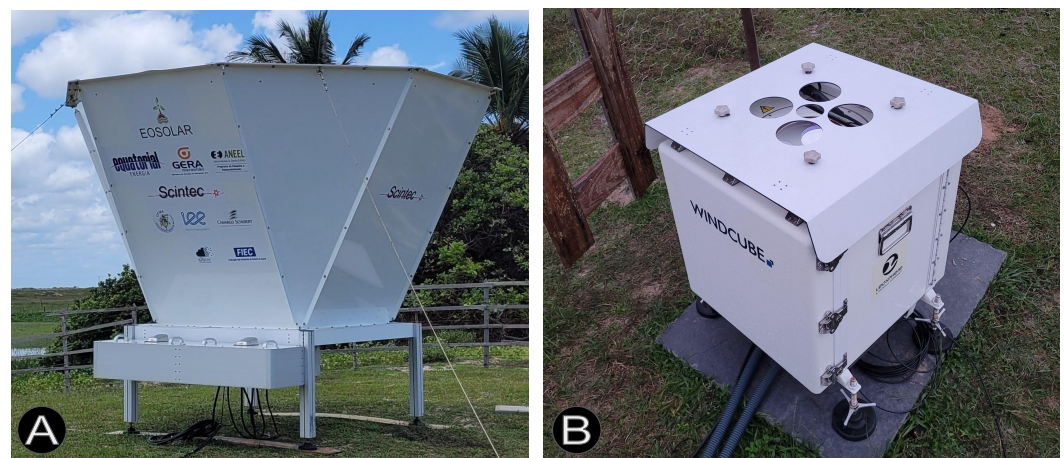


Figure 2. (A). Wind profiler SODAR MFAS, (B). Wind profiler LIDAR Windcube.

In this work, the main wind speed data used are from SODAR, as this sensor remained at the same location throughout the measurement period. To cover the periods of data unavailability, caused either by failure or maintenance, measurements from LIDAR were used. This sensor moved between four stations; the farthest one was about 3 km from SODAR's location (red circle in Figure 1). Figure 3 illustrates the data from both sensors and the merged version at 130 m, which is the hub height of the wind generator that is used in this work. Finally, to cover the intervals in which measurements were unavailable from both sensors, an autoregressive fitting function was applied using the last and the next 140 samples from the data gap. The black squares highlight the periods where data from LIDAR were used to fill unavailability gaps, and the red squares highlight the periods where none of the sensors were available.

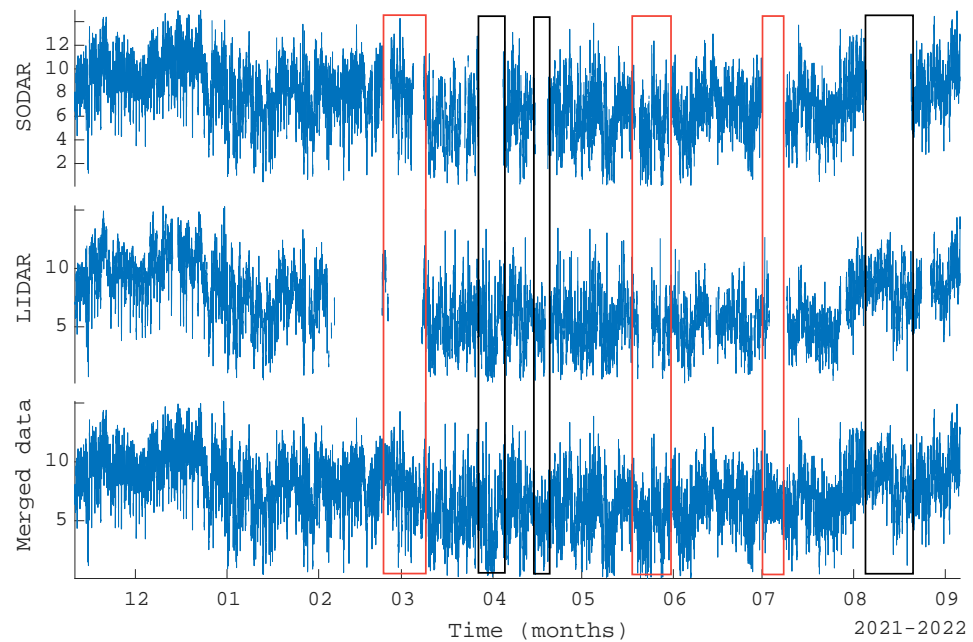


Figure 3. LIDAR, SODAR and merged wind speed at 130 m height at a temporal resolution of 10 min.

In Figure 3, the seasonal variability of the wind regime present in the region can be observed. The winds are more intense in the months of July to December. This can be explained by the drier weather, which favors an increase in wind intensity due to higher atmospheric pressure gradients, combined with the northward movement of the Intertropical Convergence Zone (ITCZ), which intensifies the trade winds along the eastern coast of Maranhão [30].

As the wind speed varies along the z -axis, the turbine might receive different speeds throughout its rotor area. Hence, using only the data series at the turbine's hub height can lead to inaccuracies in the power modeling. This subject has been studied in the literature. Some authors even consider the turbulent energy to compose the wind incident on the turbine [31]. In this paper, the methodology proposed in [32], which integrates the wind speed varying in the z -axis across the swept area of the wind turbine blades, as described in Equation (2), is used to calculate an equivalent wind speed series.

$$U_{eq} = \frac{2}{A_t} \int_{H-r}^{H+r} U(z) \left(r^2 - H^2 + 2Hz - z^2 \right)^{1/2} dz \quad (2)$$

where $U(z)$ is the wind speed in (m s^{-1}) at the height z , and H , r , and A are, respectively, the hub height, the radius and the rotor area of the wind generator. These turbine parameters will be described in Section 3.3.

3.2. Solar Data

The solar irradiance measurements were performed using a sun tracker, Solys 2, manufactured by Kipp & Zonen in Delft, the Netherlands as seen in Figure 4. This device uses two moving shading balls that constantly follow the sun's position and block the direct solar radiation from being captured by two sensors, a pyrgeometer and a pyranometer. These sensors can then make a better estimation of the diffuse solar radiation. This equipment also has a pyrliometer attached to its sun tracker. Thus, it measures the direct radiation more accurately. The sum of these two characteristics in this equipment makes the estimation of the radiation reaching a photovoltaic panel more accurate than that measured only by pyranometers.



Figure 4. Solys 2 sun tracker at the measurement site.

Figure 5 presents the hourly averages for solar radiation, wind speeds at heights 80 and 190 m, and the equivalent speeds obtained through Equation (2), all normalized by their monthly max value. The seasonality seen in Figure 3 applies not only for the wind speeds, but also for the solar radiation intensity. The months with higher wind intensities are, coincidentally, the months with higher solar radiation. This aspect is negative for yearly energy complementarity. Another negative aspect of these data for energy complementarity is that in many months, for example, November and December 2021, the peaks of both sources occur at the same time. This aspect can be confirmed by Table 1. For some months, the wind speed peak is delayed from the solar radiation, such as in March 2022 and April 2022. For May, June and July of 2022, the wind decay, around 8 h local time, corresponds to an increase in solar radiation.

Table 1 presents the Pearson's correlation coefficient between the solar radiation and the equivalent wind speed for each month. According to reviews [8,33], this is the most widely used metric of complementarity between energy sources in the literature. It is a statistical metric that shows how two randomly distributed variables are related to each other. It is a value that ranges from -1 to 1 . A correlation value close to or equal to 1 represents a positive linear relationship between the variables, i.e., complementarity is minimal in this scenario. Furthermore, the correlation coefficient takes on a value of zero or close to zero when the set of values has no direct linear relationship. Finally, a coefficient with a value close to or equal to -1 indicates that the two variables are highly complementary. The only months in which the correlation coefficient is negative are June and August.

One interesting finding about these data, seen in Figure 5, is that at a height of 190 m, which is not typically measured by tower stations, there is a different pattern of diurnal variability than that observed at lower levels. At 80 m height, the wind speed peaks near noon, but as one observes higher levels (190 m), peak speeds occur during night time. In July 2022, for example, wind troughs occurred during midday, at the peak of solar radiation. Conversely, wind peaks occurred during night time. However, because this

height is not typical for commercial onshore wind turbines, the analysis will be limited to the equivalent wind series that incorporates wind speeds from 80 to 190 m.

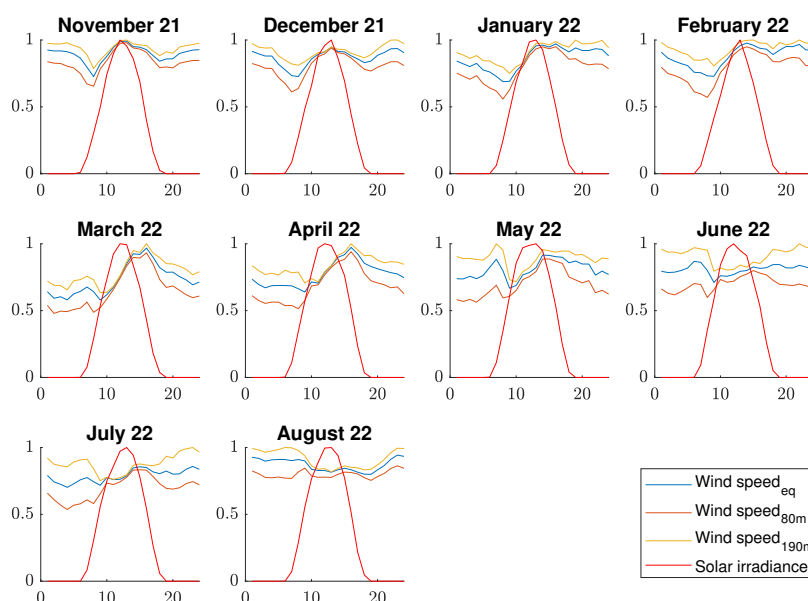


Figure 5. Monthly hourly average values of solar radiance and wind speeds, normalized to the maximum value for each respective month. The maximum hourly averages of wind speed in m s^{-1} and radiation in W m^{-2} for each month are, respectively, listed as follows: November: 10.38 and 934.36; December: 10.32 and 817.38; January: 8.53 and 802.28; February: 8.55 and 807.12; March: 7.77 and 721.46; April: 7.47 and 702.47; May: 6.77 and 677.36; June: 8.34 and 727.88; July: 9.16 and 801.27; August: 9.54 and 906.14.

Table 1. Pearson's correlation coefficient between solar radiation and equivalent wind speed.

November	December	January	February	March	April	May	June	July	August
0.3912	0.2344	0.1925	0.1979	0.3311	0.2545	0.0536	−0.5451	0.0951	−0.5311

Figure 6 presents the monthly averages for wind and solar radiation, normalized by 9.28748 m s^{-1} and 266.96 W m^{-2} . The correlation coefficient between these two data series is equal to 0.7229, indicating poor complementarity of resources on a seasonal scale. It happens that dry weather, in addition to providing an increase in the wind regime in the region, is also a relevant scenario for the reduction of clouds, which increases the amount of solar radiation reaching the surface.

In conclusion, there is no complementarity of solar and wind resources on a monthly time scale, but there is weak complementarity on a diurnal scale, with some months demonstrating correlations $r \leq 0$ (Table 1). Therefore, our analysis will answer the question of whether it is viable to hybridize a plant based on the Brazilian regulation of hybrid plants. The economic complementarity between these two sources in the composition of a grid-connected hybrid power plant will be explored.

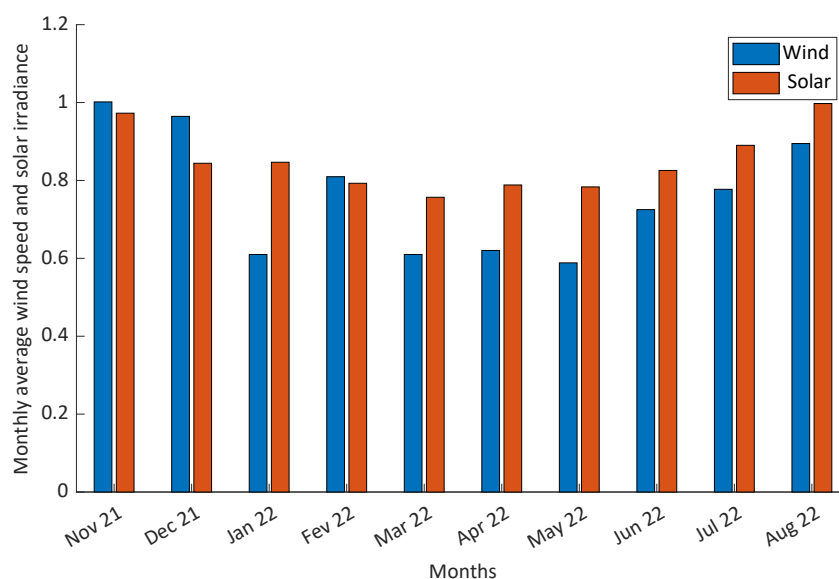


Figure 6. Monthly average normalized solar radiation and equivalent wind speed.

3.3. Wind Conversion

For the conversion of wind speed into electrical power, the curve of the wind turbine power (W) as a function of wind speed (m s^{-1}) is used, represented by $P_{\text{wind}} = f(U_{\text{eq}})$. A Siemens 2.3-113 turbine manufactured by Siemens Gamesa Renewable Energy (SGRE) Zamudio, Spain, was used for the power calculation, as it is similar to the model used in the Delta III wind park, the GE Energy 2.3-116 manufactured by GE Energy, Schenectady, New York, USA. Unfortunately, the power curve of the GE 2.3-116 turbine was not available. Table 2 lists the technical specifications of the Siemens 2.3-113 and compares them to the GE 2.3-116.

Table 2. Specification of the turbine and comparison with the model used in the nearby wind farm.

Turbine Comparison		
Manufacturer	GE Energy	SGRE
Model	2.3-116	2.3-113
Rated power (MW)	2.3	2.3
Rotor diameter (m)	116	113
Swept area (m^2)	10,569	10,000
Specific area (m^2/kW)	4.6	4.3
Number of blades	3	3
Power control	Pitch	Pitch
Cut-in wind speed (m s^{-1})	3	3
Rated wind speed (m s^{-1})	10.4	10.5
Cut-off wind speed (m s^{-1})	22	25.0

Using the power curve provided by the manufacturer, a degree 20 polynomial was generated. Figure 7 compares the curve provided by the manufacturer with the curve generated by the polynomial using the same wind speed input data. Visual analysis shows that the degree of fidelity between the real and modeled curves is high.

3.4. Solar Conversion

The PV panel model chosen for the energy conversion in the solar PV modeling is a bifacial BiHiKu7 670MB-AG, manufactured by Canadian Solar, Guelph, Ontario, Canada. Table 3 lists the technical specifications of this PV module.

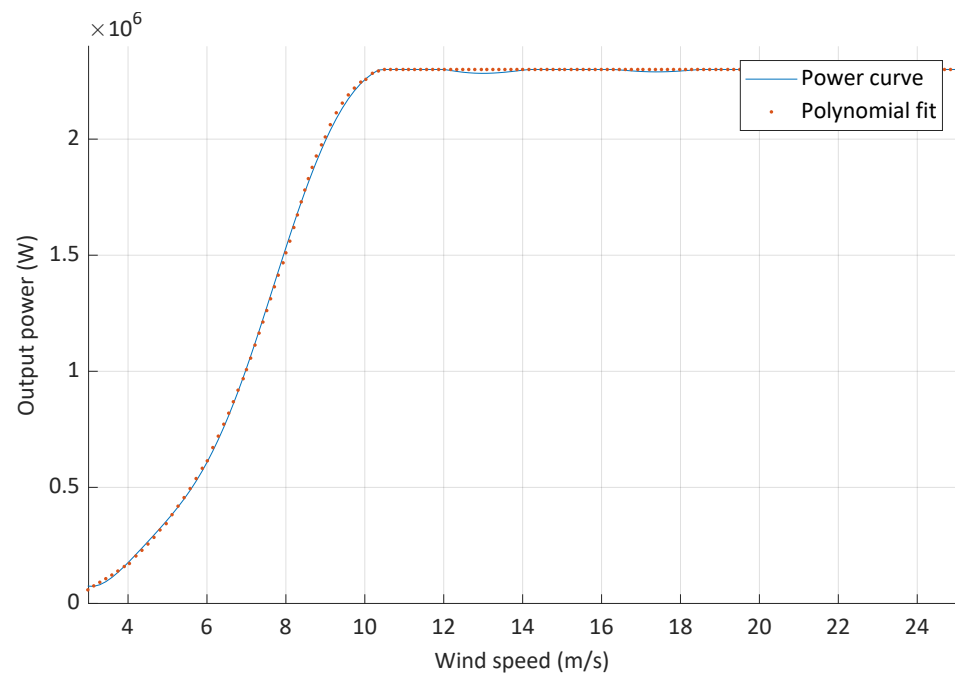


Figure 7. Siemens 2.3-113 power curve.

Table 3. Photovoltaic Solar Panel Specifications.

Canadian Solar BiHiKu7 670MB-AG	
Rated Power	804 W
Module Efficiency	25.90%
Maximum power current	20.78 A
Maximum power voltage	38.7 V
Area	3.1
Cell Type	Mono-crystalline
Dimensions	2384 × 1303 × 35 mm
Power Bifaciality	70%
Operating Temperature	41 ± 3 °C

As the efficiency, nominal power, and area of the panels are known, the solar power generated by the plant at instant (i) is determined by multiplying the number of panels. When the solar radiation is greater than or equal to 1000 W/m^2 , the panel output will be equal to its nominal power, as shown in Equation (3).

$$P_{solar} = \begin{cases} P_r, & \text{if } G(i) \geq 1000; \\ \eta A_{PV} G(i), & \text{otherwise.} \end{cases} \quad (3)$$

where:

P_r is the rated power of the solar panel;

P_{solar} is the power output of the panel;

η corresponds to the conversion efficiency;

A_{PV} is the area of the photovoltaic panel (m^2);

and $G(i)$ is the irradiance received by the panel (W m^{-2}) at instant i .

For simplification in modeling, the following assumptions related to wind and solar generation were made:

- Wind generators act in all directions of wind flow.
- As the wind direction is predominantly northeast, no stops for machine rotation are considered.

- All the conversion devices (turbines and PV panels) that compose the power plant receive the same wind speed and the same amount of solar radiation.
- The panel always works at its nominal efficiency.
- As the study region is located at 5 degrees to the equator, losses relative to the inclination of the panel were not considered.
- The temperature at which the solar panel operates is always considered constant and ideal.
- No wake effects or periods of maintenance for wind turbines are considered.

3.5. Power Plant

The total installed power of all the plant configurations modeled in the optimization process is equal to 23 MW. This decision meets the criteria of the REN no. 77 of 18 August 2004 for the reduction of tariffs for the use of the transmission and distribution systems for renewable generation projects with power injected into the system less than or equal to 30 MW. It is also the same nominal power as the majority of the wind farms that compose the Delta III complex. To assess the impact caused by varying the proportion between sources, all plant configurations need to respect the power balance equation described in Equation (4) (i.e., when the percentage of one source increases, the other source decreases in the same proportion, and vice versa). Therefore, the sum of the capacity of both sources is always constant, as seen in Equation (4).

$$P_{total} = P_{wind} + P_{solar} \quad (4)$$

where:

P_{total} is the total installed power of the power plant;

P_{wind} is the installed power of wind generation;

P_{solar} is the installed power of solar PV generation.

In the composition of the modeled hybrid plants, the power flow generated by the two sources occurs at the same connection point. Therefore, it is considered that they are part of the same generation plant.

3.6. Physical Guarantee

Decree no. 5.163/2004 establishes that the maximum amount of energy that a plant can commercialize through contracts in the SIN (National Interconnected System) is equal to the physical guarantee of that generation unit. To calculate the physical guarantee, an annual energy occurrence criterion is applied: P_{90} for wind energy and P_{50} for solar energy. Losses in the plant are subtracted from these values, and the result is divided by the number of hours in a year, as shown in Equations (5) and (6).

$$PG_{wind} = \frac{P_{90}(1 - EFOR)(1 - PU) - \Delta P}{8760} \quad (5)$$

$$PG_{sol} = \frac{P_{50}(1 - EFOR)(1 - PU) - \Delta P}{8760} \quad (6)$$

where: PG_{wind} and PG_{sol} are the wind and solar physical guarantee in W_{avg} ;

P_{90} and P_{50} are the annual energy production with an incidence equal to 90% for wind generation and 50% for solar generation in MWh/year;

$EFOR$ is the equivalent forced outage rate in pu;

PU is the programmed unavailability in pu;

ΔP is the annual estimate of internal consumption and electrical losses in MWh;

and 8760 is the number of hours in a year.

For wind farms, the probability of occurrence criterion applied is P_{90} . This means that the energy that can be commercialized needs to occur on at least 90% of the days in an estimated year. For solar generation, on the other hand, the P_{50} criterion is applied.

Analogously to P_{90} , the estimated power to be marketed needs to occur on at least 50% of the days. This difference is due to the fact that these sources have different intermittency profiles. The solar source is only available during part of the day, while the wind resource is accessible for 24 h per day. This variation in availability is also seen seasonally, as, in the rainiest periods, the solar irradiation is lower.

The graph in Figure 8 shows the daily generation in MWh, from 2.3 MW capacity, of each source for all 300 days of operation modeled. The data were then placed in decreasing order. The P90 marker for wind generation was placed at 90% of the period, and the P_{50} marker for solar was set at 50% of the period. As these data represent the amount of daily energy that both sources can generate in 50 and 90% of the analyzed period, in terms of the physical guarantee, it is necessary to divide this number by 24. The unit for this energy parameter is average power W_{avg} . In order to arrive at the amount of energy that the plant can sell in auctions, this number must be multiplied by the time, in hours, that the plant will work. The physical guarantee for solar energy is $560 kW_{avg}$, and for wind it is $548 kW_{avg}$.

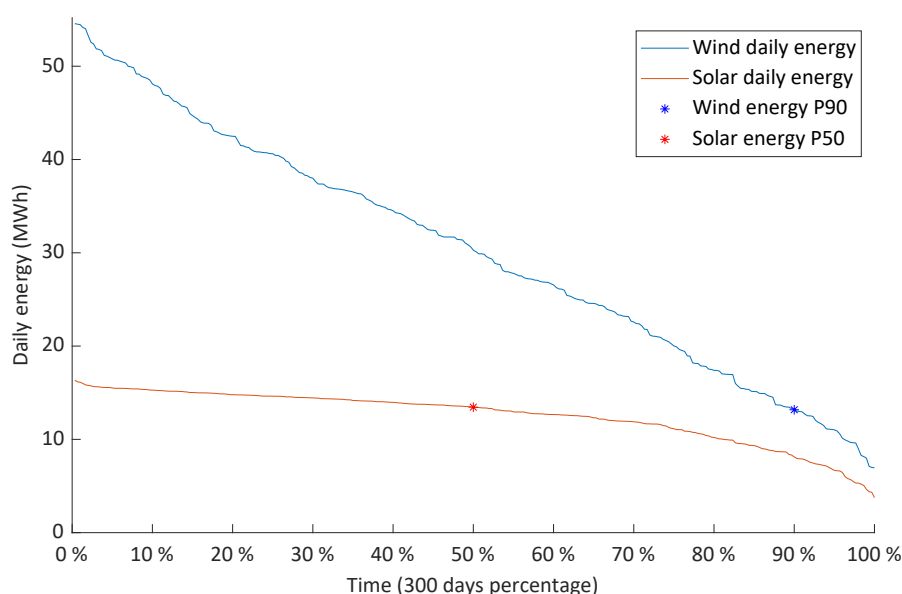


Figure 8. Energy annual P90 for wind generation and P50 for solar.

Finally, REN 954 establishes that the physical guarantee of a hybrid plant will be the sum of each physical guarantee for each source weighted by the percentage composition of each source. Thus, increasing the percentage of a source with a higher physical guarantee would also increase this characteristic for the entire hybrid plant.

4. Optimal Wind–Solar Ratio

REN 954 was created with the intention of encouraging hybrid generation enterprises. This new resolution makes it possible to choose the TSAU contracted by the enterprise, this number mandatorily being within the power range. This possibility raises the need for a definition of two important variables in the hybrid plant project.

- The proportion between each one of the sources.
- The TSAU contracted on a permanent basis so that the enterprise can reduce its expenses with EUST and transmit the largest possible amount of its generation.

Because these values depend on how much each source generates in the whole period, they depend on the characteristics of the region in which the plant is installed. In this work, two metaheuristics will be used to determine the optimal ratio between the installed power of each source and the contracted TSAU value that maximizes the plant's profit from energy sales while reducing its EUST based on measured solar irradiance and wind speed data.

4.1. Metaheuristic

For the optimization, the GA metaheuristic will be used. This algorithm is a classic and widely employed in the literature [34], and its detailed description will not be provided in this paper. The parameters utilized in the implementation are listed in Table 4.

Table 4. Genetic algorithm parameters.

GA Parameters	
Population size	50
Max _{it}	200
Crossover	0.1
Σ mutation	0.01
μ mutation	0.02

4.2. Objective Function

The algorithm works with the objective of profit maximization. In this work, the profit is composed of the amount received from the sale of energy in the free market added to the amount received from the sale of energy in auctions subtracted from the TSUC. Two constraints are applied: the first one is that the sum of the installed capacities, P_{total} , is constant, and the second is that the capacity of the contracted transmission system, P_{trans} , must always be greater than or equal to the installed capacity of the predominant source in the plant, P_{main} , and less than or equal to the sum of the installed capacities of all sources that comprise the plant, P_{total} .

$$\begin{aligned}
 &\text{Maximize Revenue} = \text{Sale}_{\text{auctions}} + \text{Sale}_{\text{FreeMarket}} - \text{TSUC} \\
 &\text{Subject to} \\
 &\begin{cases} P_{\text{solar}} + P_{\text{wind}} = P_{\text{total}} \\ P_{\text{total}} \geq P_{\text{trans}} \geq P_{\text{main}}, \end{cases}
 \end{aligned} \tag{7}$$

where P_{solar} is the solar power capacity, P_{wind} is the wind power capacity, P_{total} is the power capacity of the plant, P_{trans} is the percentage of the power capacity that is contracted for the transmission system, and P_{main} is the power capacity of the dominant technology that composes the hybrid plant.

The fee charged for the use of the transmission system was considered to be 0.9 \$/kWmonth, which was the value practiced in the state of Ceará in 2022. The energy sale values were those practiced in the A-5 energy auction (30 September 2021), and for the free market, the average price of 2022, as listed in Table 5, was considered. The exchange rate used to convert Brazilian currency, BRL, into American currency, USD, is from 21 December 2020, which was 1 USD = 5.18 BRL.

Table 5. Energy pricing.

	Energy Auction (\$)	Free Energy Market (\$)
Wind energy	33.8	10.75
Solar energy	36.9	10.75

The sales prices at auctions are higher than those in the free market, so the most logical strategy for an enterprise aiming at higher profits would be to sell all its production at auctions. Law 10,848/04, regulated by art. 2 of Decree 5163/04, establishes that the amount of energy that a plant can commercialize through auctions, including imports, is equal to its physical guarantee. In Section 3.6, it was seen that the physical guarantee of solar generation is slightly higher than that of wind generation. In addition to a higher physical guarantee, the energy generated from solar sources has higher selling prices in comparison with wind sources. On the other hand, solar energy, because it is not produced at night,

has a lower capacity factor and consequently generates less energy when compared to wind energy. These aspects increase the complexity of the problem. The algorithm should calculate the entire annual operation of the plant for several configurations of wind and solar power and TSAU before finding the most profitable solution.

5. Results

As REN 954 specifies that transmission contracts should be signed for a period of 4 years with the possibility of annual adjustments, it would be logical to use a one-year data period to determine the optimal percentage between the sources in the plant. However, with the aim of examining the effects of seasonality in the region, the algorithm was executed monthly. After the monthly analysis, a year-long analysis was conducted to determine the optimal configuration of the plant. Table 6 presents the results achieved in terms of the optimal percentage of installed power from each source, transmission contracting percentage, profit in USD, and the number of iterations required by the algorithm to reach this result. Once again, because the installed capacity of the power plant cannot be modified every month to meet the monthly optimality criterion, this analysis focuses on examining how the algorithm behaves seasonally.

Table 6. Optimization results.

	November	December	January	February	March	April	May	June	July	August
Revenue (USD)	2,011,253	1,275,877	919,315	920,080	502,590	518,404	489,346	661,934	7,762,945	1,418,636
Wind (%)	100	100	100	100	46.34	40.55	40.00	66.30	74.77	100
Solar (%)	0	0	0	0	53.65	59.44	59.99	33.69	25.22	0
TSAU (%)	100	100	100	100	59.13	59.44	59.99	66.30	74.77	100
Iterations	1	1	1	1	42	49	35	46	41	1

In the months of November, December, January, February and August, the configuration that generates the highest profit for these market conditions maintains the plant with wind power alone. These months are, coincidentally, the months with the highest incidence of wind and solar irradiance. It happens that, in this period, wind generation is so expressive that the transmission costs lose relevance in view of the values obtained. In this period, the algorithm prioritizes the source that has the highest CF and that generates energy during the whole day.

The five months in which the algorithm proposes hybridization of the plant, March–July, are coincidentally those in which the average solar irradiance and wind speed, as seen in Figure 5, are lower. In this period, as energy generation is lower, the TSUC becomes relevant when compared to the profits obtained from the sale of energy. The strategy of hybridizing the plant to reduce transmission costs becomes viable in this scenario of lower generation. This is evidenced by the reduction in the TSAU, which was normalized by the 23 MW nominal power of the plant, as the solar power increases in the hybrid plant.

Due to the fact that hybridization was only proposed by the algorithm in 5 months of the analyzed period, the analysis will be continued solely for this period. Table 7 compares the power generated from the plant in three different cases: pure wind, pure solar, and profit-optimized hybrid electricity generation following the wind–solar rate seen in Table 6. It is important to note that all values are normalized to the pure wind case for each month.

It is noticeable that the hybridization process actually leads to a reduction in energy production when compared to the wind-only case. In April, for example, there was a 22% reduction in energy production after the optimization. This reduction in energy production proposed by the optimization to maximize profits is mainly due to the low complementarity between the sources during these months, as listed in Table 1. An expected behavior for complementary sources would be an increase in energy production after the optimization.

Table 7. Energy results.

	Wind Energy (%)	Solar Energy (%)	Optimized Energy (%)
March	100.00	61.56	79.38
April	100.00	63.07	78.04
May	100.00	68.93	81.36
June	100.00	51.10	83.52
July	100.00	45.57	86.27

To verify whether, even with the reduction in energy production, the algorithm was able to find configurations that deliver higher profit, Table 8 compares the profits for the same three cases. Again, the values are normalized to the pure wind case.

July was the month that had the highest profit gain with hybridization. As the TSAU in this month is equal to 74.77% of the installed power, any generation that occurs above this value cannot be transmitted and should be cut. The last column of the table shows the energy curtailment percentage. The month that presented the highest curtailment was March, with a value of approximately 1%, for a profit increase of more than 1%.

Table 8. Profit results.

	Wind Profit (%)	Solar Profit (%)	Optimized Profit (%)	Energy Curtailment (%)
March	100.00	98.06	117.08	0.97
April	100.00	83.26	110.37	0.79
May	100.00	67.70	105.01	0.46
June	100.00	127.30	132.78	0.36
July	100.00	138.16	139.15	0.55

Finally, the efficiency of the TSUC is evaluated, using a metric proposed in [35] called IAMUST. Similarly to CF, it indicates the efficiency of the transmission contract. A value equal to 1 indicates that 100% of the transmission contract is being used. The calculation of IAMUST is described by Equation (8). Here, this metric is called transmission system capacity factor or CF_{trans} .

$$CF_{trans} = \frac{\sum_0^n P_i - PC_i}{nTSAU} \quad (8)$$

where:

P_i = Power output of the plant at instant i (MW);

PC_i = Excess power cut off at instant i . That is, in case TSUC is exceeded, this value corresponds to the difference between the output power and the TSAU (MW). When TSAU is not exceeded, this value will be null;

n = the total number of samples.

Table 9 presents the CF_{trans} values for the three cases previously analyzed, and in the last column, the CF_{trans} gain achieved by the optimization. In all months in which hybridization occurred, there was a gain in CF_{trans} . The optimization brought a gain of up to 35% (in the month of May) in the efficiency of the transmission contract. In all five months, there would be a CF_{trans} reduction if the plant was only solar. The hybrid option is the most efficient, transmission-wise, in all cases.

Table 9. Transmission system contract efficiency results. Optimization gain refers to the percentage of improvement of CF_{trans} relative to CF_{trans} for wind.

	CF_{trans} Wind	CF_{trans} Solar	Optimized CF_{trans}	Optimization Gain (%)
March	0.33	0.20	0.44	34.23
April	0.33	0.21	0.44	31.26
May	0.30	0.21	0.41	35.60
June	0.43	0.22	0.54	25.96
July	0.52	0.24	0.60	15.37

Finally, for the annual analysis, the GA optimization was run for the entire analyzed period, with an increase in solar price sales varying from 10 to 40% compared with the prices in Table 5. The algorithm was executed for the entire year, considering each 1% increase in pricing. The results, including solar ratio, profit, and TSUC, are summarized in Figure 9.

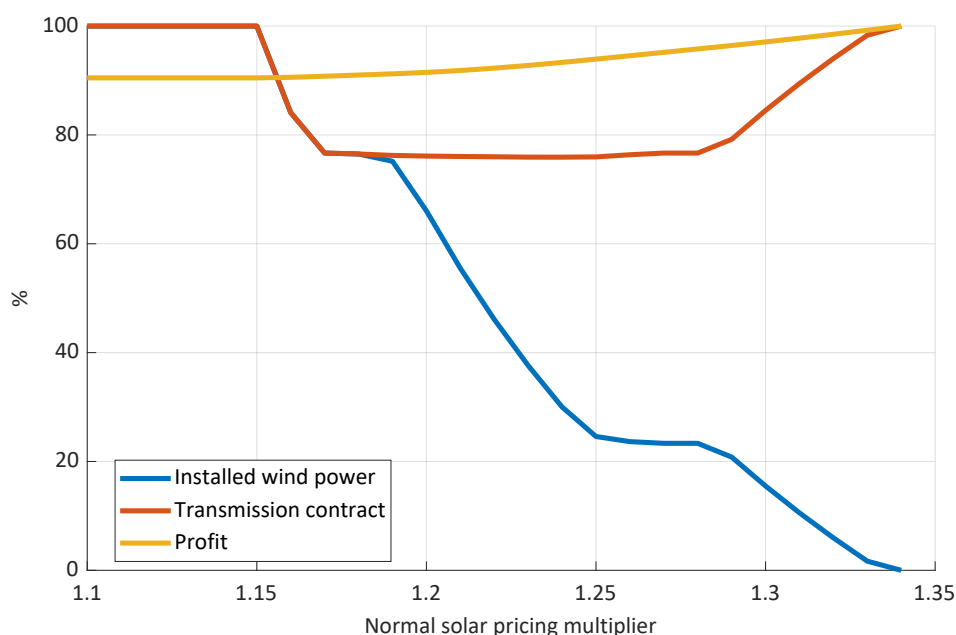


Figure 9. Power plant sensibility to solar energy price increase.

For the market situation analyzed, the optimizer indicates a non-hybrid plant with a power capacity of 100% wind. As the selling value of solar energy increases, so does its competitiveness when compared to wind energy. For a price increase of 15%, the profit-optimized configuration changes to hybrid, with approximately 20% solar energy in the composition and a TSUC equal to the wind capacity. The profit, which in this graph is normalized to the maximum value achieved, shows a slight increase with this hybridization. One point to emphasize is that, if there were a 34% increase in solar energy pricing, the most profitable plant configuration would be entirely solar PV. In this scenario, the profit increase would be about 10%.

6. Conclusions

In this work, the complementarity of a hybrid plant is evaluated by optimizing the wind–solar ratio for grid-connected hybrid plants under the Brazilian regulations. Although regulations require contracts to be signed for a period of 4 years, with the possibility of changes each year, the algorithm was run for monthly operation. Although the sources do not show complementarity according to the Pearson coefficient metric, solutions were achieved that increase profit by up to 39% with the hybridization of the plant when compared to the pure wind case. As the hybrid solutions allow transmission contracting below

capacity, all hybrid solutions proposed by the algorithm come with a cut of up to 1% of the monthly energy generated. In all of the hybrid solutions, in addition to the increase in profit, there was also an increase in the efficiency of transmission contracts.

As a result of a quick analysis of Table 9, one can notice that hybridization improves efficiency in the use of a transmission system during the months studied. The increase in the CF_{trans} allied to the reduction in the contract opens the possibility of installing more generation capacity using the same transmission structure. This solution brings advantages for the power plant, as it reduces the cost of transmission system contracting per MW of installed capacity.

The main simulation that determines the optimal plant configuration is the annual one. The results show that the wind and solar radiance characteristics, added to the regulatory conditions and market prices prevailing at the time of the publication of this paper, were not enough to encourage the deployment of hybrid plants in the region. However, a slight increase in solar energy pricing would change this scenario, which proves that the methodology applied here works. A government incentive to increase the efficiency of the transmission system or a fluctuation in prices, for example, would make a hybrid plant an optimal solution.

In this work, due to the expectation of weak temporal complementarity between the sources due to local climatic characteristics, economic complementarity (i.e., when, taking into consideration local regulations, one or more sources complement each other, bringing economic benefits or advantages to the power generation system entrepreneur) was explored. The results of the study demonstrate that, whether through increased profit in monthly analysis or improved efficiency of the transmission system contract, the region is capable of exploiting economic complementarity between the sources, bringing real benefits to the generating agent. In other words, although temporal complementarity may suggest the infeasibility of hybridization, economic complementarity opens the potential and incentive for hybridization or the installation of hybrid power plants.

Author Contributions: Conceptualization, R.B.S.V., C.B.M.O., S.L.d.L., O.R.S. and D.Q.O.; Data curation, R.B.S.V., C.B.M.O., D.Q.O. and F.M.P.; Formal analysis, R.B.S.V., C.B.M.O., S.L.d.L. and F.M.P.; Funding acquisition, O.R.S. and D.Q.O.; Investigation, R.B.S.V., C.B.M.O., S.L.d.L. and O.R.S.; Methodology, R.B.S.V., C.B.M.O., S.L.d.L., O.R.S., D.Q.O. and F.M.P.; Project administration, D.Q.O.; Supervision, O.R.S.; Validation, R.B.S.V. and C.B.M.O.; Writing—original draft, R.B.S.V. and C.B.M.O.; Writing—review & editing, R.B.S.V., C.B.M.O., O.R.S., D.Q.O., F.M.P., D.C.P.L., A.R.T.J., F.L.A.N., R.M.d.F. and A.T.A. All authors have read and agreed to the published version of the manuscript.

Funding: The authors acknowledge funding from Equatorial Energia and Gera Maranhão under the Brazilian National Electric Energy Agency's (ANEEL) R&D Program (PD-00037-0042/2020), the National Council for Scientific and Technological Development of Brazil (CNPq), the Foundation for Support to Research and Scientific and Technological Development of Maranhão (FAPEMA), Coordination for the Improvement of Higher Education Personnel (CAPES), and the National Institute of Science & Technology in Ocean and Fluvial Energies (INEOF).

Data Availability Statement: The data presented in this study are available on request from the corresponding author. The data are not publicly available due to confidentiality agreements of the EOSOLAR project.

Acknowledgments: This study was supported by the Brazilian Electricity Regulatory Agency (ANEEL) under the R&D project (PD-00037-0042/2020), funded by Gera Maranhão S.A. and Equatorial Energia S.A. The authors also acknowledge support from the National Council for Scientific and Technological Development of Brazil (CNPq), the Foundation for Support to Research and Scientific and Technological Development of Maranhão (FAPEMA), Coordination for the Improvement of Higher Education Personnel (CAPES), and the National Institute of Science & Technology in Ocean and Fluvial Energies (INEOF). We are thankful to Gilberto Feitosa and Dalila Porto for continuous support and cooperation.

Conflicts of Interest: The authors declare no conflicts of interest.

Abbreviations

VRES	Variable Renewable Energy Sources
LIDAR	Light Detection and Ranging
SODAR	Sound Detection and Ranging
GA	Genetic Algorithm
BESS	Battery Energy Storage Systems
ANEEL	Brazilian Electricity Regulatory Agency
CUST	Contracts of Use of the Transmission System
REN	Normative Resolution
TSAU	Transmission System Amount of Use
TSUC	Transmission System Use Charge
TSUF	Transmission System Use Fee
HPP	Hybrid Power Plant
ITCZ	Intertropical Convergence Zone
CNPq	National Council for Scientific and Technological Development of Brazil
FAPEMA	Foundation for Support to Research of Maranhão
CAPES	Coordination for the Improvement of Higher Education Personnel
INEOF	National Institute of Science & Technology in Ocean and Fluvial Energies
$U(z)$	Wind speed in (m s^{-1}) at the height z
U_{eq}	Wind speed equivalent
H	The hub height of the wind generator
r	The radius of the wind generator
A	The area of the wind generator
P_r	The rated power of the solar panel
P_{solar}	The power output of the panel
η	Panel conversion efficiency
A_{PV}	The area of the photovoltaic panel (m^2)
$G(i)$	Solar irradiation at instant i
P_{total}	The total installed power of the power plant
P_{wind}	The installed power of wind generation
P_{solar}	The installed power of solar PV generation
PG_{wind}	The solar physical guarantee
PG_{sol}	The wind physical guarantee
EFOR	The programmed unavailability in pu
ΔP	The annual estimate of internal consumption and electrical losses
P_{90}	The annual energy production with an incidence of 90%
P_{50}	The annual energy production with an incidence of 50%
P_{trans}	The capacity of the contracted transmission system
P_{main}	The installed capacity of the predominant source in the plant
$Sale_{auctions}$	The amount received from the sale of energy in auctions
$Sale_{FreeMarket}$	The amount received from the sale of energy in the free market
P_i	Power output of the plant at instant i
PC_i	Excess power cut off at instant i
n	The total number of samples
CF_{trans}	The capacity factor of the transmission system contract

References

1. BP. Statistical Review of World Energy. 2021. Available online: <https://www.bp.com/en/global/corporate/energy-economics/statistical-review-of-world-energy.html> (accessed on 12 December 2022).
2. Sulaeman, S.; Tian, Y.; Benidris, M.; Mitra, J. Quantification of Storage Necessary to Firm Up Wind Generation. *IEEE Trans. Ind. Appl.* **2017**, *53*, 3228–3236. [CrossRef]
3. Kini, R.; Raker, D.; Stuart, T.; Ellingson, R.; Heben, M.; Khanna, R. Mitigation of PV Variability Using Adaptive Moving Average Control. *IEEE Trans. Sustain. Energy* **2020**, *11*, 2252–2262. [CrossRef]
4. Chen, X.; Du, Y.; Xiao, W.; Lu, S. Power ramp-rate control based on power forecasting for PV grid-tied systems with minimum energy storage. In Proceedings of the IECON 2017—43rd Annual Conference of the IEEE Industrial Electronics Society, Beijing, China, 29 October–1 November 2017; IEEE 2017; pp. 2647–2652.

5. Majumder, S.; Khaparde, S.A.; Agalgaonkar, A.P.; Ciufu, P.; Perera, S.; Kulkarni, S. DFT-based sizing of battery storage devices to determine day-ahead minimum variability injection dispatch with renewable energy resources. *IEEE Trans. Smart Grid* **2017**, *10*, 626–638. [\[CrossRef\]](#)
6. Hart, E.K.; Stoutenburg, E.D.; Jacobson, M.Z. The potential of intermittent renewables to meet electric power demand: Current methods and emerging analytical techniques. *Proc. IEEE* **2011**, *100*, 322–334. [\[CrossRef\]](#)
7. Kahn, E. *Reliability of Wind Power From Dispersed Sites: A Preliminary Assessment*; Energy and Environment Division, Lawrence Berkeley Laboratory: Berkeley, CA, USA, 1978.
8. Jurasz, J.; Canales, F.; Kies, A.; Guezgouz, M.; Beluco, A. A review on the complementarity of renewable energy sources: Concept, metrics, application and future research directions. *Sol. Energy* **2020**, *195*, 703–724. [\[CrossRef\]](#)
9. Guezgouz, M.; Jurasz, J.; Chouai, M.; Bloomfield, H.; Bekkouche, B. Assessment of solar and wind energy complementarity in Algeria. *Energy Convers. Manag.* **2021**, *238*, 114170. [\[CrossRef\]](#)
10. Castro, R.; Crispim, J. Variability and correlation of renewable energy sources in the Portuguese electrical system. *Energy Sustain. Dev.* **2018**, *42*, 64–76. [\[CrossRef\]](#)
11. Lopez-Rey, A.; Campinez-Romero, S.; Gil-Ortego, R.; Colmenar-Santos, A. Evaluation of supply–demand adaptation of photovoltaic–wind hybrid plants integrated into an urban environment. *Energies* **2019**, *12*, 1780. [\[CrossRef\]](#)
12. Couto, A.; Estanqueiro, A. Exploring wind and solar PV generation complementarity to meet electricity demand. *Energies* **2020**, *13*, 4132. [\[CrossRef\]](#)
13. François, B.; Hingray, B.; Raynaud, D.; Borga, M.; Creutin, J. Increasing climate-related-energy penetration by integrating run-of-the river hydropower to wind/solar mix. *Renew. Energy* **2016**, *87*, 686–696. [\[CrossRef\]](#)
14. Canales, F.A.; Jurasz, J.; Beluco, A.; Kies, A. Assessing temporal complementarity between three variable energy sources through correlation and compromise programming. *Energy* **2020**, *192*, 116637. [\[CrossRef\]](#)
15. Rosa, C.D.O.C.S.; Costa, K.A.; Christo, E.D.S.; Bertahone, P.B. Complementarity of hydro, photovoltaic, and wind power in Rio de Janeiro State. *Sustainability* **2017**, *9*, 1130.
16. Neto, P.B.L.; Saavedra, O.R.; Oliveira, D.Q. The effect of complementarity between solar, wind and tidal energy in isolated hybrid microgrids. *Renew. Energy* **2020**, *147*, 339–355. [\[CrossRef\]](#)
17. Han, S.; Zhang, L.n.; Liu, Y.q.; Zhang, H.; Yan, J.; Li, L.; Lei, X.h.; Wang, X. Quantitative evaluation method for the complementarity of wind–solar–hydro power and optimization of wind–solar ratio. *Appl. Energy* **2019**, *236*, 973–984. [\[CrossRef\]](#)
18. Silva, A.R.; Estanqueiro, A. From Wind to Hybrid: A Contribution to the Optimal Design of Utility-Scale Hybrid Power Plants. *Energies* **2022**, *15*, 2560. [\[CrossRef\]](#)
19. Miglietta, M.M.; Huld, T.; Monforti-Ferrario, F. Local complementarity of wind and solar energy resources over Europe: an assessment study from a meteorological perspective. *J. Appl. Meteorol. Climatol.* **2017**, *56*, 217–234. [\[CrossRef\]](#)
20. Risso, A.; Beluco, A.; Marques Alves, R.D.C. Complementarity roses evaluating spatial complementarity in time between energy resources. *Energies* **2018**, *11*, 1918. [\[CrossRef\]](#)
21. Mareda, T.; Gaudard, L.; Romerio, F. A parametric genetic algorithm approach to assess complementary options of large scale windsolar coupling. *IEEE/CAA J. Autom. Sin.* **2017**, *4*, 260–272. [\[CrossRef\]](#)
22. Fürsch, M.; Hagspiel, S.; Jägemann, C.; Nagl, S.; Lindenberger, D.; Tröster, E. The role of grid extensions in a cost-efficient transformation of the European electricity system until 2050. *Appl. Energy* **2013**, *104*, 642–652. [\[CrossRef\]](#)
23. Schaber, K.; Steinke, F.; Mühlich, P.; Hamacher, T. Parametric study of variable renewable energy integration in Europe: Advantages and costs of transmission grid extensions. *Energy Policy* **2012**, *42*, 498–508. [\[CrossRef\]](#)
24. Steinke, F.; Wolfrum, P.; Hoffmann, C. Grid vs. storage in a 100% renewable Europe. *Renew. Energy* **2013**, *50*, 826–832. [\[CrossRef\]](#)
25. Bolinger, M.; Gorman, W.; Rand, J.; Wiser, R.H.; Jeong, S.; Seel, J.; Warner, C.; Paulos, B. *Hybrid Power Plants: Status of Installed and Proposed Projects*; Lawrence Berkeley National Laboratory: Berkeley, CA, USA, 2021.
26. Gallardo, R.P.; Ríos, A.M.; Ramírez, J.S. Analysis of the solar and wind energetic complementarity in Mexico. *J. Clean. Prod.* **2020**, *268*, 122323. [\[CrossRef\]](#)
27. ENTSO-E. Overview of Transmission Tariffs in Europe: Synthesis 2020. 2021. Available online: https://eepublicdownloads.entsoe.eu/clean-documents/mc-documents/l_entso-e_TTO-Report_2020_03.pdf (accessed on 12 December 2022).
28. Torres Junior, A.R.; Saraiva, N.P.; Assireu, A.T.; Neto, F.L.; Pimenta, F.M.; de Freitas, R.M.; Saavedra, O.R.; Oliveira, C.B.; Lopes, D.C.; de Lima, S.L.; et al. Performance Evaluation of LIDAR and SODAR Wind Profilers on the Brazilian Equatorial Margin. *Sustainability* **2022**, *14*, 14654. [\[CrossRef\]](#)
29. Assireu, A.T.; Pimenta, F.M.; de Freitas, R.M.; Saavedra, O.R.; Neto, F.L.; Júnior, A.R.T.; Oliveira, C.B.; Lopes, D.C.; de Lima, S.L.; Veras, R.B.; et al. EOSOLAR Project: Assessment of Wind Resources of a Coastal Equatorial Region of Brazil—Overview and Preliminary Results. *Energies* **2022**, *15*, 2319. [\[CrossRef\]](#)
30. Fernandes, I.; Pimenta, F.M.; Saavedra, O.R.; Assireu, A.T. Exploring the Complementarity of Offshore Wind Sites to Reduce the Seasonal Variability of Generation. *Energies* **2022**, *15*, 7182. [\[CrossRef\]](#)
31. Wharton, S.; Lundquist, J.K. Atmospheric stability affects wind turbine power collection. *Environ. Res. Lett.* **2012**, *7*, 014005. [\[CrossRef\]](#)
32. Sumner, J.; Masson, C. Influence of Atmospheric Stability on Wind Turbine Power Performance Curves. *J. Sol. Energy Eng.* **2006**, *128*, 531–538.

33. Weschenfelder, F.; Leite, G.d.N.P.; da Costa, A.C.A.; de Castro Vilela, O.; Ribeiro, C.M.; Ochoa, A.A.V.; Araujo, A.M. A review on the complementarity between grid-connected solar and wind power systems. *J. Clean. Prod.* **2020**, *257*, 120617. [[CrossRef](#)]
34. Papazoglou, G.; Biskas, P. Review and Comparison of Genetic Algorithm and Particle Swarm Optimization in the Optimal Power Flow Problem. *Energies* **2023**, *16*, 1152. [[CrossRef](#)]
35. Veras, R.B.; Chaves, A.A.; Oliveira, C.B.; Oliveira, D.Q.; Saavedra, O.R.; de Lima, S.L.; Cortes, D.O. Exploração da Complementaridade Eólica-Solar no Uso Eficiente dos Contratos de Uso do Sistema de Transmissão de Energia Elétrica. In Proceedings of the Simpósio Brasileiro de Sistemas Elétricos-SBSE, Santa Maria, Brazil, 10–13 July 2022; Volume 2.

Disclaimer/Publisher’s Note: The statements, opinions and data contained in all publications are solely those of the individual author(s) and contributor(s) and not of MDPI and/or the editor(s). MDPI and/or the editor(s) disclaim responsibility for any injury to people or property resulting from any ideas, methods, instructions or products referred to in the content.